gels

Article

Design and Optimization of Thermosensitive Hydrogels Combined with Lipid Nanotechnology for Topical Curcumin Application

Daniela Vergara [1,2,*], Benjamín Vega [2,3], Claudia Sanhueza [4,5], Mariela Bustamante [6,7,8], Francisca Acevedo [1,2,9] and Olga López [10]

1 Center of Excellence in Translational Medicine—Scientific Technological Bioresource Nucleus (CEMT-BIOREN), Laboratory of Pharmaceutical and Cosmetic Bioproducts, Faculty of Medicine, Universidad de La Frontera, Temuco 4811230, Chile
2 Millennium Nucleus Bioproducts, Genomics and Environmental Microbiology (BioGEM), Avenida España 1680, Valparaíso 2390123, Chile
3 Chemistry and Pharmacy Undergraduate Program, Faculty of Medicine, Universidad de La Frontera, Temuco 4811230, Chile
4 Center for Resilience, Adaptation and Mitigation (CReAM), Universidad Mayor, Temuco 4780000, Chile
5 Escuela de Ingeniería, Facultad de Ciencias, Ingeniería y Tecnología, Universidad Mayor, Temuco 4780000, Chile
6 Center of Food Biotechnology and Bioseparations—BIOREN, Universidad de La Frontera, Temuco 4811230, Chile
7 Centre of Biotechnology and Bioengineering (CeBiB), Universidad de La Frontera, Temuco 4811230, Chile
8 Centro de Excelencia en Investigación Biotecnológica Aplicada al Medio Ambiente (CIBAMA), Universidad de La Frontera, Temuco 4811230, Chile
9 Department of Basic Sciences, Faculty of Medicine, Universidad de La Frontera, Temuco 4811230, Chile
10 Department of Chemical and Surfactant Technology, Institute of Advanced Chemistry of Catalonia (IQAC-CSIC), C/Jordi Girona 18–26, 08034 Barcelona, Spain
* Correspondence: daniela.vergara@ufrontera.cl

Abstract

A novel co-encapsulation platform based on curcumin-loaded liposomes (Cur-Lip) incorporated into thermosensitive hydrogels (TSH) was developed to address the physicochemical and biological limitations of topical curcumin (Cur) delivery. Response Surface Methodology (RSM) was used to optimize Pluronic® F-127, glycerol, and alginate concentrations with respect to gelation time and viscosity. The optimized formulation (22% Pluronic® F-127, 5% glycerol, and 0.5% alginate) exhibited rapid time sol–gel transition (~86 s), suitable viscosity (~377 mPa·s), excellent model fitting (R^2 = 0.99) and prediction accuracy. Three formulations (TSH, Cur-TSH, and Cur-Lip-TSH) were subsequently prepared and displayed appropriate thermoresponsive behavior. The Cur-Lip system showed high encapsulation efficiency (~78%). Upon incorporation into the TSH, Cur-Lip-TSH displayed increased viscosity and mechanical strength at physiological temperature. In vitro studies confirmed its cytocompatibility toward human keratinocytes, significant antibacterial activity against *Staphylococcus aureus*, *Staphylococcus epidermidis*, and *Pseudomonas aeruginosa*, and no irritation potential as assessed by the Hen's Egg Test on the Chorioallantoic Membrane assay (HET-CAM). Overall, Cur-Lip-TSH represents a safe and robust thermosensitive platform that provides a foundation for future studies on controlled curcumin release and topical performance.

Keywords: thermosensitive hydrogel; liposome; curcumin; delivery system; topical administration

Academic Editors: Maddalena Sguizzato and Rita Cortesi

Received: 15 January 2026
Revised: 6 February 2026
Accepted: 18 February 2026
Published: 20 February 2026

1. Introduction

Hydrogels are three-dimensional networks of water-insoluble polymer chains (natural or synthetic) characterized by high equilibrium water content, mechanical softness, biocompatibility, oxygen permeability, temperature sensitivity, and the potential for either chemical stability or controlled degradation [1]. These properties make hydrogels highly attractive for biomedical applications, particularly in drug delivery. However, hydrogel-based delivery systems still face important challenges, such as burst release at the site of administration, low encapsulation efficiency for certain therapeutic agents (such as hydrophobic molecules, proteins, or antibodies), and difficulties in conforming to the complex geometry of the *stratum corneum* [2].

To overcome these limitations, hydrogels can be engineered to provide sustained drug release profiles, which help reduce dosing frequency and improve patient compliance [3]. Two main strategies have been proposed to enhance their performance in topical drug delivery. The first strategy focuses on the development of stimuli-responsive hydrogels capable of releasing active agents in response to specific physical, chemical, or biological cues, including changes in temperature, pH, light, enzymatic activity, or oxidative conditions [4,5]. The second approach involves incorporating nanocarriers into the hydrogel matrix to improve stability and controlled release of therapeutic compounds [6].

In relation to the first strategy, thermosensitive and pH-responsive hydrogels have gained particular interest for topical applications, as the skin microenvironment naturally exhibits fluctuations in these parameters. Thermosensitive hydrogels (TSH) undergo a sol-to-gel transition upon reaching a critical temperature, typically referred to as the lower critical solution temperature (LCST). At this point, polymer chains change their conformation from a coil-like to a globular state [7]. Below the LCST, hydrogel exists in a low-viscosity sol state, facilitating application. Above this temperature, it forms a semi-solid gel that remains localized at the site of administration, enabling controlled release [5].

Among the various thermosensitive gelling agents, Poloxamers—commercially known as Pluronic®—are triblock copolymers composed of polyethylene and polypropylene oxides (PEO–PPO–PEO) and are among the most extensively studied. Their amphiphilic nature and reversible thermal behavior make them excellent candidates for in situ gelation at physiological temperatures [8]. To further enhance the performance of Pluronic®-based hydrogels, a variety of additives have been explored, including glycerol [9], chitosan [10], hyaluronic acid [11], alginate [12], hydroxypropyl methylcellulose [13], Carbopol® [14], Polysorbate [15], and other Pluronic® variants [16]. Among these, glycerol and alginate have demonstrated significant potential for topical applications. Glycerol functions as a humectant, emollient, and skin protectant [17], while alginate contributes to the formation of a biocompatible and bioadhesive matrix [18].

Regarding the second strategy, combining hydrogels with lipid-based nanocarriers has been proposed to enhance drug stability and improve skin permeation. Liposomes (Lip) are biocompatible, spherical nanoparticles composed of one or more phospholipid bilayers enclosing an aqueous core. This structure enables the encapsulation of hydrophilic, hydrophobic, and amphiphilic drugs, protecting them from physiological degradation and prolonging their half-life. The structural versatility of Lip supports the development of tailored drug delivery platforms adapted to specific therapeutic needs [19]; Many studies have shown the potential of Lip for topical dermal application [20,21].

Beyond improving drug stability and biocompatibility, the integration of lipid nanocarriers into TSH enables the development of multilevel delivery systems, in which the TSH controls macroscopic properties such as application and retention [3], while nanocarriers modulate drug protection and release behavior [21]. This architecture provides a

rational basis for controlled drug availability over time and on the site of application in topical formulations.

A compound of particular interest for this type of delivery system is curcumin (Cur), a bioactive polyphenol extracted from *Curcuma longa*. Cur has been widely investigated for the treatment of various skin conditions due to its potent antioxidant, anti-inflammatory, antimicrobial, and wound-healing activities [22,23]. However, its clinical utility is limited by low aqueous solubility (less than 0.1 mg/mL), rapid degradation under physiological conditions, low skin permeability, and the potential for yellow staining or local irritation [24,25], which greatly limits its clinical application.

Although no previous studies have specifically addressed the integration of a Cur-loaded Lip system (Cur-Lip) into a TSH (Cur-Lip-TSH) composed of Pluronic® F-127, glycerol, and alginate, several related systems have demonstrated promising outcomes. Notably, we have previously developed Cur encapsulation strategies in lipid-based systems combining Lip and bicelles, achieving high encapsulation efficiencies exceeding 75% [26]. In addition, Chen et al. [20] reported that Cur-loaded nanostructured lipid carriers (NLC) within an in situ TSH enhanced skin permeation and exhibited significant anti-inflammatory activity without causing irritation. Histological analysis further confirmed improved drug penetration across the *stratum corneum*, highlighting the potential of this system for dermal Cur delivery. Similarly, Zhang et al. [27] reported that a Cur-Lip gel formulated with sodium alginate improved bioavailability and antioxidant capacity, offering effective protection against UV-induced skin damage by reducing oxidative stress and enhancing superoxide dismutase (SOD) activity. Additionally, Agrawal et al. [28] demonstrated that Cur-loaded solid lipid nanoparticles, optimized using response surface methodology (RSM) and incorporated into a TSH, exhibited favorable physicochemical characteristics and a biphasic, diffusion-controlled drug release profile.

The development of novel carrier systems and dosage forms requires careful consideration of multiple formulation variables, and their optimization is essential to ensure desirable quality attributes in the final product. In this context, the application of design of experiments methodologies is highly valuable. Among them, RSM provides a faster, more cost-effective alternative to traditional single-variable or full factorial approaches for hydrogel optimization. This statistical tool allows for the simultaneous evaluation of individual and interactive effects among formulation parameters, with a relatively low prediction error, making it widely applicable in experimental design [29].

Unlike previously reported Cur-Lip gels or NLC-based TSH systems, which typically incorporate nanocarriers into pre-formed gel matrices, the present study addresses the systematic multivariate optimization of a Pluronic® F-127/glycerol/alginate TSH using an RSM–Central Composite Design (CCD), specifically tailored for the incorporation of Cur-Lip. This formulation-focused approach prioritizes a balanced combination of gelation behavior, viscosity, biological safety (cytotoxicity and irritation), and antibacterial performance, thereby establishing a well-characterized platform for subsequent topical delivery studies.

2. Results and Discussion

2.1. Experimental Design and Data Analysis

In this study, the influence of the independent variables X_1: Pluronic® F-127 concentration (% *w*/*w*), X_2: glycerol concentration (% *w*/*w*), and X_3: alginate concentration (% *w*/*w*), as well as their interactions, was evaluated on the formulation responses Y_1, gelling time (s), and Y_2, viscosity (mPa·s). Gelling time (Y_1) was measured at 34 ± 1 °C, corresponding to the approximate skin surface temperature [30], whereas viscosity (Y_2) was determined at room temperature (22 ± 1 °C).

The experimental conditions for the 16 runs and the corresponding experimental and predicted response values are summarized in Table 1, showing good agreement between experimental and predicted data and stable pH values across all formulations. To illustrate the interactions among the variables and the relationship between factor levels and each response, three-dimensional response surface plots for gelling time and viscosity are shown in Figure 1a–f, revealing that gelling time is mainly influenced by Pluronic® F-127 concentration, whereas viscosity is predominantly governed by alginate content, with glycerol exerting a secondary modulatory effect.

Table 1. Central composite design (CCD) with experimental and predicted gelling time and viscosity values of the thermosensitive hydrogel (TSH).

				Gelling Time at 34 °C (s)		Viscosity at 22 °C (mPa·s)		pH
Run	**X_1**	**X_2**	**X_3**	**Experimental Value**	**Predicted Value**	**Experimental Value**	**Predicted Value**	
1	20	2.5	0.2	209 ± 8	213.42	85 ± 1	94.07	6.39 ± 0.02
2	22	2.5	0.2	132 ± 3	126.13	93 ± 3	99.56	6.78 ± 0.02
3	20	5	0.2	203 ± 4	205.13	81 ± 5	75.28	6.40 ± 0.02
4	22	5	0.2	115 ± 6	110.28	97 ± 1	103.49	6.52 ± 0.01
5	20	2.5	0.5	217 ± 1	220.13	317 ± 10	317.07	6.62 ± 0.03
6	22	2.5	0.5	117 ± 5	113.27	324 ± 2	336.15	6.67 ± 0.02
7	20	5	0.5	190 ± 6	194.44	332 ± 5	332.89	6.72 ± 0.00
8	22	5	0.5	86 ± 1	80.02	377 ± 3	374.69	6.62 ± 0.05
9	19.3	3.75	0.35	279 ± 11	269.70	165 ± 4	166.07	6.37 ± 0.03
10	22.7	3.75	0.35	89 ± 7	100.09	216 ± 3	205.84	6.54 ± 0.10
11	21	1.64	0.35	169 ± 6	169.61	195 ± 4	181.56	6.47 ± 0.04
12	21	5.85	0.35	134 ± 5	134.68	194 ± 4	198.18	6.41 ± 0.04
13	21	3.75	0.09	146 ± 7	148.13	72 ± 2	65.08	6.36 ± 0.02
14	21	3.75	0.60	128 ± 2	128.33	484 ± 0.4	480.65	6.52 ± 0.04
15	21	3.75	0.35	166 ± 5	167.85	211 ± 10	209.32	6.55 ± 0.02
16	21	3.75	0.35	170 ± 10	167.85	206 ± 4	209.32	6.58 ± 0.01

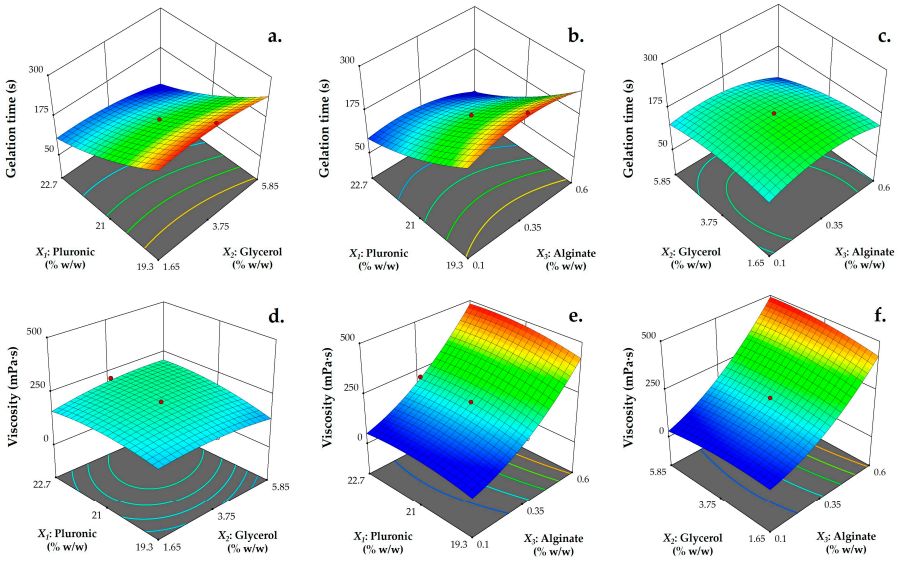

Figure 1. Response surface plots illustrating the effects of Pluronic® F-127 (X_1), glycerol (X_2), and alginate (X_3) concentrations (% *w*/*w*) on gelling time (**top**) and viscosity (**bottom**) of the thermosensitive hydrogel (TSH). The graphs illustrate the interaction between: (**a**,**d**) X_1 and X_2, (**b**,**e**) X_1 and X_3, and (**c**,**f**) X_2 and X_3, with the third variable held constant at its central value. Color gradients indicate predicted responses and red dots represent experimental data points.

2.1.1. Effect of Independent Variables on Gelling Time

The statistical significance of the coefficients in the quadratic model for gelling time (s), as determined by ANOVA, is summarized in Table 2. The model was highly significant ($p < 0.0001$), with a coefficient of determination $R^2 = 0.99$ and an adjusted $R^2 = 0.98$, indicating that the model accurately explains the variability in the response. The coefficient of variation (CV = 5.01) further supports the reliability and reproducibility of the experimental design.

Table 2. Analysis of variance (ANOVA) and regression coefficients between response variables gelling time (s) and viscosity (mPa·s), and the independent variables: X_1, Pluronic® F-127 concentration (% *w*/*w*) X_2, glycerol concentration (% *w*/*w*), and X_3, alginate concentration (% *w*/*w*) used for elaboration of thermosensitive hydrogel (TSH).

	Gelling Time at 34 °C (s)				Viscosity at 22 °C (mPa·s)			
Source	**DF**	**Coefficient**	**Sum of Squares**	***p* Value**	**DF**	**Coefficient**	**Sum of Squares**	***p* Value**
Model	9	167.85	39,509.18	<0.0001	9	209.32	2.214×10^5	<0.0001
X_1	1	−50.43	34,727.75	<0.0001	1	11.82	1909.42	0.0078
X_2	1	−10.39	1473.09	0.0030	1	4.94	333.20	0.1529
X_3	1	−5.89	473.39	0.0344	1	123.55	2.085×10^5	<0.0001
X_1X_2	1	−1.89	28.63	0.5276	1	5.68	258.10	0.1999
X_1X_3	1	−4.89	191.43	0.1337	1	3.40	92.25	0.4224
X_2X_3	1	−4.35	151.38	0.1741	1	8.65	599.16	0.0707
X_1^2	1	6.03	336.56	0.0612	1	−8.26	632.08	0.0651
X_2^2	1	−5.55	285.51	0.0786	1	−6.88	437.92	0.1098
X_3^2	1	−10.47	1015.88	0.0072	1	22.47	4675.96	0.0009
Residual	6		382.18		6	209.32	746.83	
Lack of Fit	5		374.18		5	11.82	729.23	
Pure error	1		8.00		1		17.60	
Total	15		39,891.36		15		2.221×10^5	
R^2		0.99				0.99		
Adj-R^2		0.98				0.99		
CV		5.01				5.18		

DF: Degrees of freedom.

Among the evaluated factors, Pluronic® F-127 concentration (X_1) exhibited the strongest influence on gelling time, with a highly significant and negative coefficient (−50.43, $p < 0.0001$), indicating that increasing this component markedly reduces the gelling time. Glycerol concentration (X_2) also showed a significant, though less pronounced, negative effect ($p = 0.0030$), possibly by influencing the hydration dynamics of the system. Notably, the linear term of alginate concentration (X_3) was statistically significant ($p = 0.0344$), indicating that alginate exerts a direct influence on gelling behavior within the studied range.None of the interaction terms (X_1X_2, X_1X_3, X_2X_3) showed statistical significance ($p > 0.05$), indicating that the effects of the individual formulation variables on gelling time were predominantly independent. Regarding quadratic terms, X_3^2 exhibited a significant effect ($p = 0.0072$), revealing a nonlinear contribution of alginate concentration to gelation behavior. In contrast, the quadratic terms X_1^2 and X_2^2 were not statistically significant ($p > 0.05$).

The experimental results indicate that increasing concentrations of Pluronic® F-127 and glycerol significantly reduce gelling time, whereas alginate exhibits a nonlinear influence on this parameter. This trend is consistent with the intrinsic thermosensitive behavior of Pluronic® F-127, which undergoes a liquid–gel transition under room and physiological conditions when the system exceeds the critical micelle concentration (CMC) or critical mi-

cellization temperature (CMT). At low temperatures, individual PEO–PPO–PEO polymer chains remain homogeneously dispersed in solution; however, as temperature increases, progressive dehydration of the PPO blocks drives micelle formation, characterized by a hydrophobic PPO core and a hydrophilic PEO corona [11]. Subsequent micellar interactions and corona entanglement promote network formation, ultimately leading to gelation at the critical gelation temperature (CGT) [31]. Consistent with previous reports, higher Pluronic® F-127 concentrations favor the formation of a larger micellar population, thereby reducing both the temperature and time required for the sol–gel transition [32]. In this context, formulations containing < 10% (*w*/*w*) Pluronic® exhibit low CMC, resulting in dispersed micelles that do not fully organize into a stable core–shell structure. In contrast, concentrations around ≥ 20% (*w*/*w*) are considered suitable for topical applications on irritated or wounded skin, as they remain fluid at room temperature and are easily applied whereas higher concentrations promote dense micellar networks that may hinder application on damaged skin [11].

In the present formulation, glycerol incorporation was associated with modifications in gelation kinetics. Previous studies suggest that glycerol molecules may localize at the micelle–water interface, inducing microstructural rearrangements within the hydrogel network that favor faster gelation [33]. Comparable effects have been reported in chitosan–Poloxamer 407 hybrid hydrogels, where physical interactions between polymeric chains facilitated micelle aggregation and reduced gelation time [13]. Supporting these findings, Lee et al. [34] described silk-fibroin-based thermosensitive hydrogels incorporating glycerol and Pluronic® F-127, demonstrating that glycerol improved control over gelation kinetics and mechanical strength, while Pluronic® F-127 enabled rapid sol–gel transition at physiological temperatures.

From a practical perspective, reduced gelation time is advantageous for topical applications, as it ensures the rapid formation of a semi-solid layer upon skin contact. This behavior enhances formulation retention at the application site and promotes the sustained release of bioactive compounds embedded within the hydrogel matrix, thereby improving therapeutic efficacy [35].

2.1.2. Effect of Independent Variables on Viscosity

The statistical analysis of the quadratic model for viscosity (mPa·s) is presented in Table 2. The model was found to be highly significant ($p < 0.0001$), with a coefficient of determination $R^2 = 0.99$ and an adjusted $R^2 = 0.99$, indicating an excellent fit between the experimental and predicted values. The coefficient of variation (CV = 5.18) was low, confirming the reliability and reproducibility of the experimental data.

Pluronic® F-127 (X_1) and alginate (X_3) exhibited statistically significant positive effects on viscosity ($p = 0.0078$ and $p < 0.0001$, respectively), indicating that increasing the concentration of these components leads to higher formulation viscosity. In contrast, glycerol (X_2) did not show a statistically significant linear effect within the studied range ($p = 0.1529$).

Regarding higher-order effects, a significant quadratic contribution of alginate concentration (X_3^2) was observed ($p = 0.0009$), revealing a nonlinear influence of alginate on viscosity, potentially related to structural rearrangements or network densification at higher concentrations. In contrast, the quadratic terms X_1^2 and X_2^2, as well as the interaction terms X_1X_2, X_1X_3, and X_2X_3, did not reach statistical significance ($p > 0.05$).

Viscosity represents a fundamental parameter in the performance of topical semi-solid formulations, as it governs both the mechanical behavior of the gel and its interaction with the skin during application. The incorporation of polysaccharides such as alginate has been shown to enhance the structural integrity of hydrogels, increasing their resistance to dissolution and promoting self-healing properties [36].

Achieving an appropriate viscosity range is essential to balance formulation stability and drug release performance; excessively viscous systems may hinder penetration and diffusion, whereas low-viscosity matrices can suffer from phase separation and insufficient mechanical integrity [37].

In Pluronic-based systems, viscosity is primarily dictated by the molecular architecture of the poloxamer. Pluronic® F-127, due to its longer PPO blocks and higher hydrophobic content, forms larger and more strongly interacting micelles, resulting in a denser intermicellar network and higher bulk viscosity compared to lower–molecular weight poloxamers such as Pluronic® F-68 [38]. Nevertheless, excessively high viscosity may lead to gelation at ambient temperature (22–25 °C), which can compromise product application by spreading or spraying onto the skin [11]. In this regard, gel-state viscosities in the range of 1500 to 60,000 mPa·s have been reported as suitable for the local treatment of dermal affections [39].

Moreover, rheological properties directly influence spreadability, retention at the application site, and sensorial perception, all of which are critical determinants of patient adherence [40].

2.2. Validation of the Optimized Model

To optimize the gelation time (s) and viscosity (mPa·s), the desirability function approach was applied. The results indicated that the optimal formulation, with an overall desirability value of 0.926, corresponded to experimental run No. 8 (Table 2), consisting of 22% *w*/*w* Pluronic® F-127, 5% *w*/*w* glycerol, and 0.5% *w*/*w* alginate. Under these conditions, the predicted values for gelation time and viscosity were 80.02 s and 374.69 mPa·s, respectively.

The experimental results yielded average values of 86 ± 1 s for gelation time, corresponding to a prediction validity of 92.5%, and 377 ± 3 mPa·s for viscosity, with a prediction validity of 99.4%. These experimental outcomes were in close agreement with the values predicted by the desirability-based optimization approach, confirming the robustness and reliability of the model. Accordingly, this composition was selected for the preparation of the TSH used in subsequent studies.

2.3. Characterization of TSH, Cur-TSH, and Cur-Lip-TSH Formulations

2.3.1. Particle Size and Polydispersity Index (PDI) of Liposomes

Table 3 summarizes the particle size, PDI, and EE of unloaded Lip and Cur-Lip. The incorporation of Cur resulted in **a** non-statistically significant increase in particle size (115 ± 6 nm vs. 124 ± 13 nm), which is consistent with drug incorporation into the lipid bilayer. Both formulations exhibited low PDI values (<0.3), indicating homogeneous size distributions. The Cur-Lip system achieved an EE of 78 ± 1%, demonstrating high loading efficiency and structural stability of the vesicles.

Table 3. Particle size (nm), polydispersity index (PDI), and encapsulation efficiency (EE) of unloaded liposomes (Lip) and Cur-Lip. Each value represents the mean ± standard deviation of at least three replicates. Letter means statistically significant differences with a *p*-value < 0.05.

	Particle Size (nm)	PDI	EE (%)
Lip	115 ± 6 [a]	0.190 ± 0.04 [a]	-
Cur-Lip	124 ± 13 [a]	0.211 ± 0.06 [a]	78 ± 1

2.3.2. Macroscopic Appearance and Microstructural Analysis

The TSH, Cur-TSH, and Cur-Lip-TSH formulations were visually evaluated at room temperature and at 34 °C to confirm their sol–gel transition behavior. As shown in Figure 2a, the TSH formulation appeared as a clear, glass-like liquid without turbidity or

opalescence at room temperature. It exhibited low viscosity and flowed readily upon tilting the container, confirming its sol state. In contrast, the Cur-TSH formulation (Figure 2c) appeared yellow and transparent due to the presence of free Cur. Meanwhile, the Cur-Lip-TSH formulation (Figure 2e) presented a yellow and visibly more opaque appearance at 25 °C, with turbidity attributed to Cur-Lip. This formulation exhibited reduced transparency and a denser visual appearance, suggesting a more complex internal structure with dispersed vesicles.

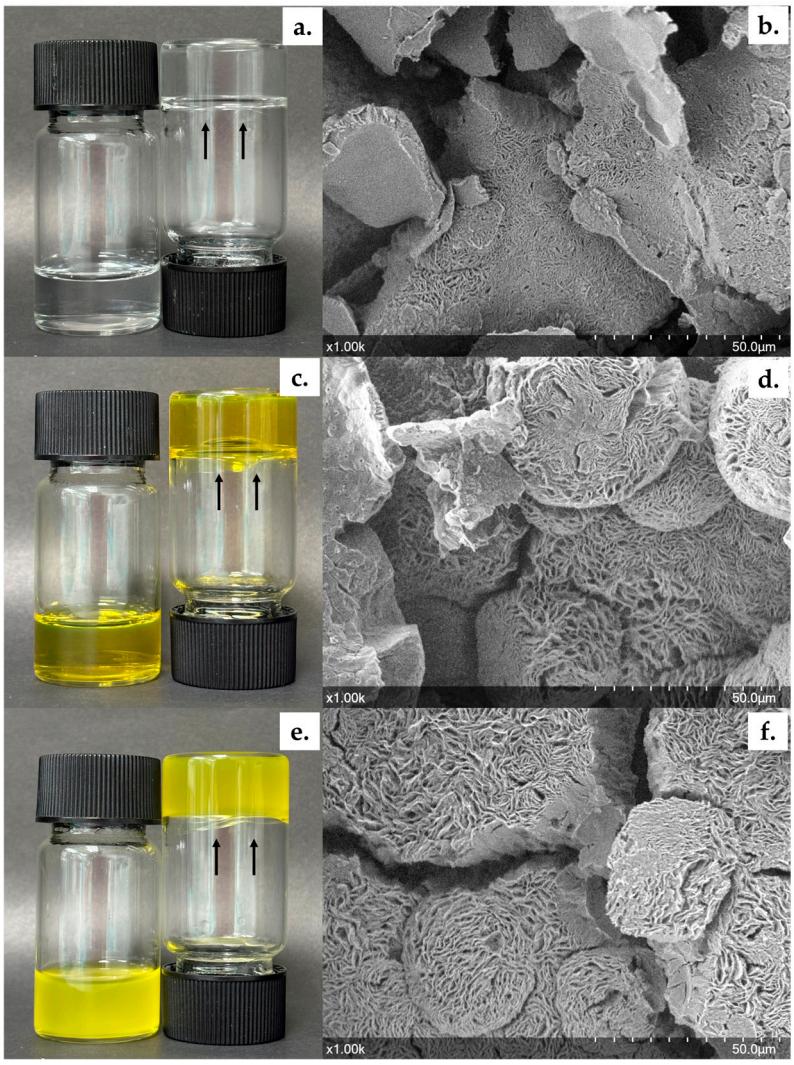

Figure 2. Visual appearance and microstructural characterization of the formulations. Macroscopic images at 25 °C (left vial) and 34 °C (right vial): (**a**) TSH, (**c**) Cur-TSH, and (**e**) Cur-Lip-TSH. Black arrows indicate the meniscus position, evidencing the sol–gel transition at physiological temperature. SEM micrographs (×1000 magnification) of freeze-dried samples: (**b**) TSH, (**d**) Cur-TSH, and (**f**) Cur-Lip-TSH. Scale bar: 50 µm.

Upon exposure to 34 °C, all systems underwent a reversible sol-to-gel transition, forming transparent or semi-transparent semi-solid gels that retained their shape and resisted gravitational flow when the vials were inverted.

This macroscopic transformation confirms the thermoresponsive nature of the hydrogel, consistent with the behavior expected from systems containing Pluronic® F-127. The addition of glycerol and alginate did not alter the optical clarity, suggesting good miscibility of components and absence of phase separation throughout the thermal transition. During storage at room temperature, no phase separation was observed, and the formu-

lation remained physically stable for at least 30 days, with no signs of destabilization or color change.

The microstructural organization of the formulations was further investigated by scanning electron microscopy (SEM) after freeze-drying. Representative SEM micrographs are shown in Figure 2b,d,f. The TSH formulation (Figure 2b) exhibited a porous morphology typical of physically crosslinked Pluronic® F-127–based hydrogels, characterized by relatively smooth and continuous domains with interconnected voids. In contrast, both the Cur-TSH (Figure 2d) and Cur-Lip-TSH (Figure 2f) formulations displayed porous networks composed of rounded structural domains embedded within the polymeric matrix, indicating that the incorporation of Cur, either in free or liposomal form, led to comparable microscale morphological features. At the magnification analyzed, the overall architecture of Cur-TSH and Cur-Lip-TSH appears largely similar; however, the Cur-Lip-TSH samples tend to exhibit more compact and densely textured rounded domains, with a more pronounced surface wrinkling. Although these differences are subtle, they may be associated with the presence and local organization of the liposomal phase within the hydrogel network.

2.3.3. Gelling Time, Viscosity, Spreadability, and pH

The gelling time and viscosity of the formulations were evaluated to characterize their performance at ambient and physiological temperatures. As shown in Table 4, all formulations exhibited rapid gelation, with gelling times ranging from 81 to 86 s, indicating a suitable sol–gel transition rate for topical application.

Table 4. Properties of the thermosensitive hydrogel (TSH) formulations. Different letters mean statistically significant differences with a p-value < 0.05.

Formulation	Gelling time at 34 °C (s)	Viscosity at 22 °C (mPa·s)	Viscosity at 34 °C (mPa·s)	Spreadability (cm^2/g)	pH
TSH	86 ± 1.0 [a]	377 ± 3.0 [b]	7552 ± 10 [b]	93 ± 3.0 [a]	7.08 ± 0.006 [a]
Cur-TSH	86 ± 1.5 [a]	368 ± 9.7 [b]	7614 ± 13 [b]	93 ± 3.0 [a]	7.08 ± 0.010 [a]
Cur-Lip-TSH	81 ± 5.7 [a]	698 ± 15 [a]	15,413 ± 23 [a]	86 ± 0.3 [b]	7.10 ± 0.012 [a]

At 22 °C, the viscosities of the TSH and Cur-TSH formulations were similar (377 ± 3.1 and 368 ± 9.7 mPa·s, respectively), while Cur-Lip-TSH displayed a markedly higher viscosity (698 ± 15 mPa·s), likely due to the incorporation of liposomes. Upon heating to 34 °C, a substantial increase in viscosity was observed for all formulations, consistent with their thermoresponsive behavior. Cur-Lip-TSH showed the highest viscosity at 34 °C (15,413 ± 23 mPa·s), more than doubling the values of TSH and Cur-TSH (7552 ± 10 and 7614 ± 13 mPa·s, respectively), highlighting its enhanced gel rigidity and structural integrity at physiological temperature. These results confirm that the inclusion of liposome-encapsulated Cur enhances the rheological properties of the hydrogel, potentially improving its retention and controlled release performance when applied to the skin.

Spreadability is a key parameter in semi-solid formulations such as gels, hydrogels, creams, or ointments, as it determines the ease of application and uniform distribution over the skin with minimal friction [41]. As a general guideline, the larger the spreading area, the better the spreadability of the formulation [42]. An effective hydrogel should spread evenly without producing any grittiness or discomfort upon application [16]. The evaluated formulations (TSH, Cur-TSH, and Cur-Lip-TSH) exhibited suitable spreadability values, confirming their appropriateness for topical use. The increasing order of spreadability was: 93 ± 3.0 cm^2/g (TSH) < 93 ± 3.0 cm^2/g (Cur-TSH) < 86 ± 0.3 cm^2/g (Cur-Lip-TSH)

(Table 4), all demonstrating homogeneous spreading with minimal shear. Generally, a spreadability greater than 9 cm^2/g is preferred for topical formulations [43].

The pH values of all tested formulations ranged around 7.0 [44], placing them near neutral (Table 4). Although these values are slightly above the typical pH of healthy skin (4.5–7.0), they remain within an acceptable range for topical use. A pH close to neutrality can help improve the solubility or stability of certain active ingredients without significantly affecting the skin's natural barrier. Overall, the pH results suggest that the TSH, Cur-TSH, and Cur-Lip-TSH formulations are compatible with the skin and appropriate for safe dermal applications.

2.3.4. Infrared Spectra (FTIR)

FTIR analysis was conducted to evaluate possible chemical interactions and functional group compatibility within the Cur-Lip-TSH formulation. The overlaid spectrum (Figure 3) revealed that the characteristic bands of the individual components (Pluronic® F-127, alginate, glycerol, Cur, cholesterol, and Lipoid P-100 were preserved in the composite system.

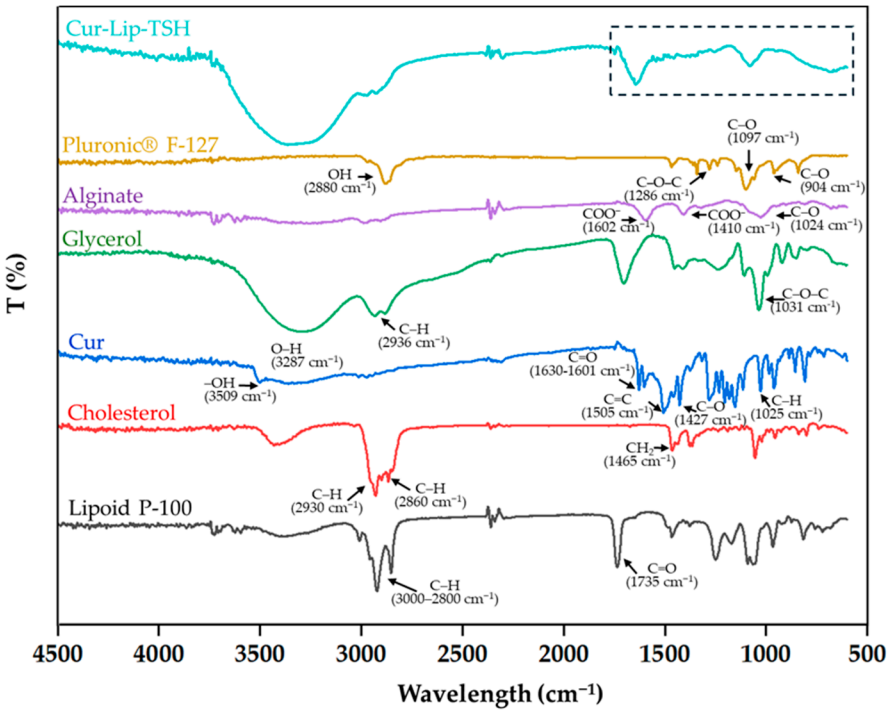

Figure 3. Fourier-transform infrared (FTIR) spectrum of the Cur-Lip-TSH formulation (–) and its individual components: Pluronic® F-127 (–), alginate (–), glycerol (–), Cur (–), cholesterol (–), and Lipoid P-100 (–).

Cur exhibited its typical absorption peaks associated with O–H and C=O stretching and aromatic C=C vibrations, confirming its structural integrity [45]. Characteristic bands of cholesterol and phospholipids (Lipoid P-100) were observed in the regions corresponding to aliphatic C–H and ester C=O groups [26], while Pluronic® F-127, glycerol, and alginate displayed their distinctive O–H, C–O and C-O-C stretching signals [46–48].

In the Cur-Lip-TSH spectrum, the well-defined characteristic peaks of Cur (1601, 1505, 1427, 1025, and 962 cm^{-1}) almost disappeared, suggesting that Cur was efficiently encapsulated within the lipid and hydrogel matrix [49]. The absence of new absorption bands or significant shifts in the 1800–900 cm^{-1} region confirms that no chemical reactions or covalent bond formation occurred, thereby preserving the chemical integrity of each component.

Overall, the FTIR results, together with the physicochemical characterization of the formulations, confirm the physical entrapment and compatibility of the Cur-Lip system within the TSH network, supporting the formation of a stable and chemically coherent formulation suitable for topical delivery.

2.4. Cell Cytotoxicity Assay

The cytotoxicity of the different formulations (TSH, Cur-TSH, and Cur-Lip-TSH), as well as free Cur dissolved in DMSO, was evaluated using an MTT assay in keratinocyte (HaCaT) cell lines. Cells were incubated for 24 h with increasing Cur concentrations ranging from 0.1 to 100 μM. For samples containing free Cur, appropriate dilutions were performed to ensure that the final DMSO concentration in contact with the cells remained below 1%, thereby minimizing potential solvent-related cytotoxic effects, while blank TSH was tested at equivalent dilution levels to those used for Cur-containing formulations.

As shown in Figure 4, cell viability exhibited a clear dependence on both Cur concentration and formulation type, with 80% viability considered the cytotoxicity threshold. Free Cur induced a pronounced cytotoxic effect at higher concentrations (100 and 50 μM); however, a progressive recovery of cell viability was observed as the concentration decreased, reaching non-cytotoxic levels at concentrations $\leq$ 10 μM. These results are consistent with previous reports indicating that free Cur exhibits higher cytotoxicity than its encapsulated counterparts. Indeed, Cur encapsulated in lipid-based systems has been shown to yield higher cell viability values than free Cur in fibroblast and keratinocyte cell lines, reflecting the reduced toxicity associated with encapsulation [50,51].

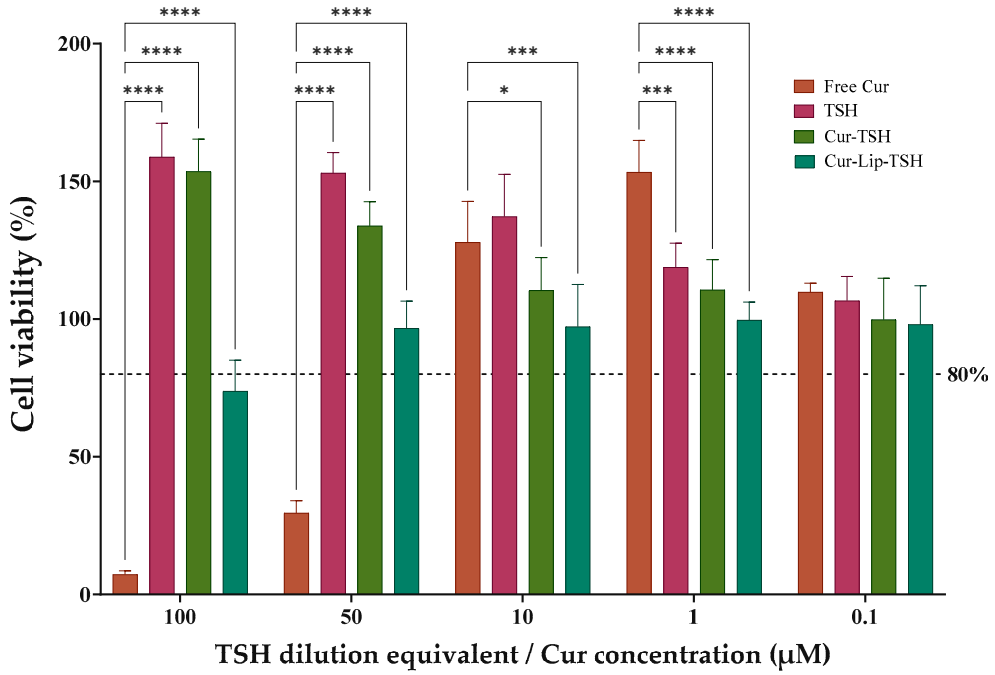

Figure 4. In vitro evaluation of cell viability of free Cur, TSH, Cur-TSH, and Cur-Lip-TSH formulations by the MTT assay for 24 h. Blank TSH was evaluated at dilution levels equivalent to those used for Cur-containing formulations to enable direct comparison. Statistical analysis of two-way ANOVA and Dunnett's multiple comparisons test: **** = $p < 0.0001$, *** = $p < 0.001$, and * = $p < 0.05$ ($n = 3$).

In contrast, TSH demonstrated excellent biocompatibility across the entire concentration range tested, with cell viability values consistently exceeding the defined threshold. Notably, cell proliferation above 100% was observed for both TSH and Cur-TSH formulations, indicating a favorable cellular response. This behavior can be attributed to the porous architecture of the hydrogel matrix, which likely facilitates nutrient diffusion, efficient

removal of metabolic waste, and improved cell adhesion, thereby promoting enhanced cell proliferation compared to the control [52].

Incorporation of Cur into the hydrogel matrix (Cur-TSH) effectively attenuated the intrinsic cytotoxicity of the free compound, maintaining cell viability above 80% even at the highest concentrations evaluated. This observation supports the role of the hydrogel network in modulating Cur bioavailability and cellular interactions. In comparison, the Cur-Lip-TSH formulation exhibited slightly increased sensitivity at 100 μM, with viability values approaching the cytotoxicity threshold; however, cell viability remained stable and clearly acceptable at concentrations $\leq$ 50 μM. This effect might be associated with the higher viscosity of the Cur-Lip-TSH system, which could locally limit oxygen diffusion, promote CO_2 accumulation, and induce minor pH fluctuations, thereby influencing cellular metabolism and proliferation [53].

Despite these formulation-dependent differences at the highest concentration tested, the overall cytocompatibility profiles of Cur-TSH and Cur-Lip-TSH were comparable, demonstrating that the incorporation of lipid nanocarriers does not compromise cellular safety while providing additional physicochemical functionality. These results suggest that the advantages of Cur-Lip-TSH may become more relevant under dynamic or prolonged application conditions, where enhanced mechanical stability and retention are expected to play a more critical role.

In line with these findings, previous studies have extensively reported the biocompatibility of Pluronic®-based hydrogels loaded with a wide range of bioactive compounds, including corticosteroids [54], cannabidiol [55], lidocaine [56], and carvedilol [57]. Consistently, systems incorporating Pluronic® F-127, liposomes, and/or Cur have been shown not to induce significant reductions in HaCaT cell viability, supporting the broader safety profile of these delivery platforms [58,59].

Beyond its safety profile, Cur is widely recognized for its wound-healing potential, attributed to its anti-inflammatory and antioxidant properties, as well as its ability to promote cell proliferation, angiogenesis, re-epithelialization, and granulation tissue formation [60]. In this context, the favorable cytocompatibility observed for Cur-TSH and Cur-Lip-TSH at therapeutically relevant concentrations supports their potential application in topical therapies aimed at skin regeneration and the management of oxidative and inflammatory skin disorders. Moreover, from a formulation perspective, the higher viscosity and gel strength of Cur-Lip-TSH at physiological temperature may further enhance retention and stability at the application site without compromising spreadability or biocompatibility.

2.5. Hen's Egg Test—Chorioallantoic Membrane (HET-CAM) Assay

The irritation potential of the prepared formulations was assessed using the Hen's Egg Test on the Chorioallantoic Membrane (HET-CAM), a well-established alternative method to in vivo ocular irritation assays. This test is widely applied as a preliminary screening tool to evaluate the irritant effects of chemical substances and topical formulations on biological membranes and skin, in accordance with the ICCVAM-recommended protocol [61] and the classification criteria proposed by Luepke [62].

The macroscopic evaluation of the CAM is presented in Figure 5. Figure 5a–e corresponds to the membranes prior to the application of the tested samples, whereas Figure 5f–j shows the same membranes after a 5 min exposure period. The negative control (0.9% NaCl) exhibited no signs of hemorrhage, vascular lysis, or coagulation, maintaining an intact vascular network throughout the observation period (Figure 5f). Accordingly, this sample obtained an irritation score of 0.0 and was classified as non-irritant (Table 5), thereby validating the reliability of the assay. In contrast, the positive control (0.1% NaOH) induced immediate and pronounced vascular damage, characterized by vessel lysis, hemorrhage,

and coagulation (Figure 5g, white arrow). This severe response resulted in a maximum irritation score of 15.0, classifying the sample as a strong irritant according to Luepke [62] and ICCVAM [61] criteria (Table 5).

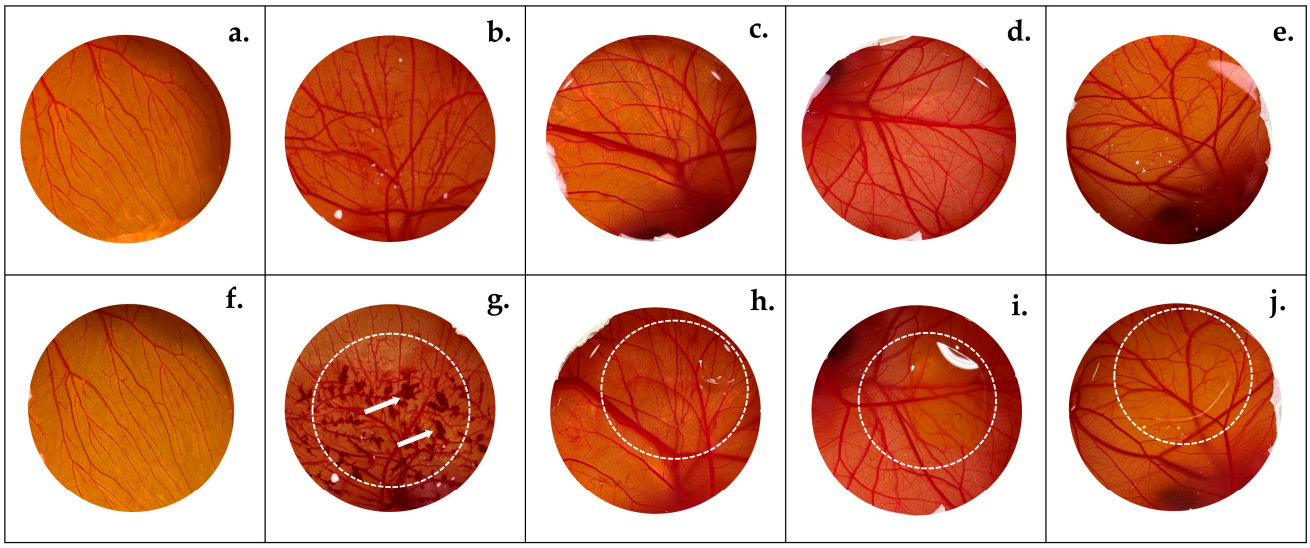

Figure 5. Evaluation of the irritant potential of the formulations before (**a**–**e**) and after (**f**–**j**) application on the chorioallantoic membrane (CAM) over a 5 min observation period. (**f**) Negative control: 0.9% NaCl, (**g**) positive control: 0.1% NaOH; (**h**) TSH formulation, (**i**) Cur-TSH formulation, and (**j**) Cur-Lip-TSH formulation. Circles indicate the formulation application sites, while arrows denote vascular damage (n = 3).

Table 5. Scores and classification of the HET-CAM irritation evaluation.

Samples	Score [a]	Classification [b]
Negative control 0.9% NaCl	0.0	Non-irritant
Positive control 0.1% NaOH	15.0	Strong irritant
TSH	0.0	Non-irritant
Cur-TSH	0.0	Non-irritant
Cur-Lip-TSH	0.0	Non-irritant

[a] ICCVAM, [61]. [b] Luepke, [62].

The irritation response of the tested formulations is shown in Figure 5h–j, where the white circle indicates the application sites. None of the formulations evaluated (TSH, Cur-TSH, and Cur-Lip-TSH) elicited detectable vascular alterations during the 5 min observation period. In all cases, the CAM preserved its structural integrity, with no evidence of hemorrhage, lysis, or coagulation. Consistent with these observations, all formulations yielded an irritation score of 0.0 and were classified as non-irritant (Table 5). Overall, the qualitative macroscopic assessment and the quantitative HET-CAM scores collectively demonstrate the absence of irritation for the developed formulations, confirming their biocompatibility and supporting their suitability and safety for topical applications.

2.6. Antibacterial Effectiveness

The antibacterial activity of TSH, Cur-TSH, and Cur-Lip-TSH was evaluated against *S. aureus*, *S. epidermidis*, and *P. aeruginosa*. As shown in Figure 6, the untreated control dis-played the highest bacterial load for all microorganisms, reflecting normal growth in the absence of any treatment. All formulations significantly reduced bacterial viability com-pared to the control ($p < 0.0001$). However, no statistically significant differences were

ob-served among TSH, Cur-TSH, and Cur-Lip-TSH, indicating that, under the experimental conditions employed, the antibacterial effect was not specifically attributable to Cur.

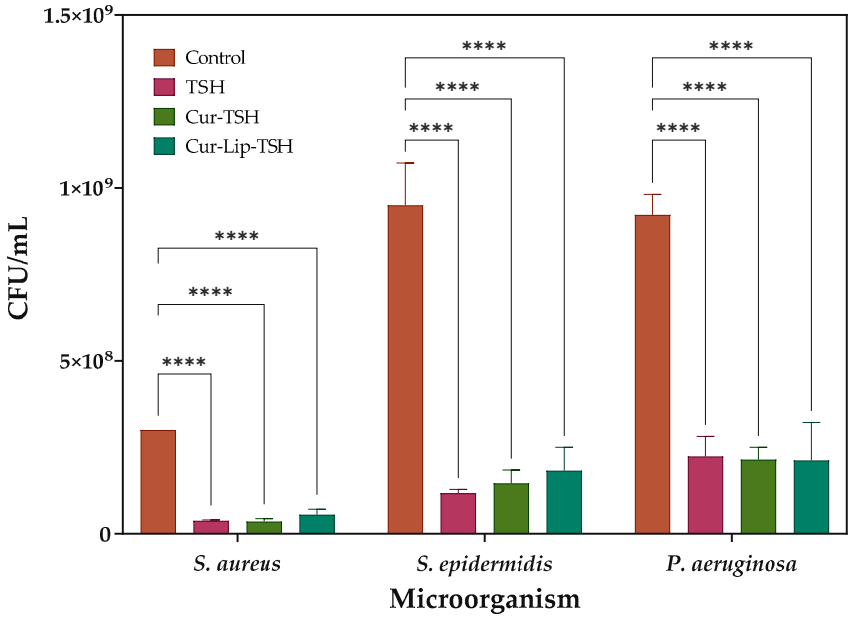

Figure 6. Antibacterial activity of the different formulations TSH, Cur-TSH, and Cur-Lip-TSH against *S. aureus*, *S. epidermidis*, and *P. aeruginosa*, expressed as CFU/mL. Statistical analysis of two-way ANOVA and Tukey's multiple comparisons test: **** = $p < 0.0001$ ($n = 3$).

This outcome is plausible in diffusion-limited in vitro assays, where antibacterial performance depends on the effective concentration of the active compound at the bacteria–material interface. Although Cur is widely reported to exhibit antimicrobial activity through mechanisms such as membrane perturbation, interference with bacterial cell division, and induction of reactive oxygen species (ROS), these effects are strongly dependent on concentration, bacterial strain, exposure time, and formulation-dependent availability [36,63–65]. In the present formulations, Cur bioavailability may be limited by its low aqueous solubility and restricted diffusion within the hydrogel matrix [66]. Moreover, in Cur-Lip-TSH, liposomal encapsulation is expected to further reduce the fraction of immediately available (free) Cur during the assay timeframe, potentially attenuating any incremental antibacterial contribution unless release is sufficiently rapid [67].

The comparable antibacterial response observed for the blank TSH formulation suggests that the hydrogel matrix itself plays a dominant role in reducing bacterial viability. While Pluronic® F-127 does not possess intrinsic bactericidal activity, it has been reported to reduce bacterial adhesion for both Gram-positive (*S. aureus*, *S. epidermidis*) and Gram-negative (*P. aeruginosa*) strains [68], thereby indirectly limiting microbial colonization and early biofilm formation. In addition, the combined polymeric network formed by Pluronic® F-127, glycerol, and alginate may hinder nutrient diffusion and metabolite exchange, contributing to growth suppression [69].

Overall, these findings position TSH as a promising material for topical applications aimed at reducing bacterial adhesion and proliferation.

3. Conclusions

In this study, a novel TSH platform incorporating Cur-loaded lipid nanocarriers (Cur-Lip-TSH) was successfully developed and optimized for topical application. The use of RSM-CCD allowed fine tuning of Pluronic® F-127, glycerol, and alginate concentrations, resulting in a formulation with rapid sol–gel transition and appropriate viscosity at

room and physiological temperature. The incorporation of lipid nanocarriers increased the mechanical strength and structural integrity of the hydrogel while preserving its thermoresponsive behavior.

Although Cur-TSH and Cur-Lip-TSH demonstrated comparable cytocompatibility and safety profiles, the inclusion of lipid nanocarriers provided additional functional value by improving gel consistency and mechanical robustness, and by establishing a structural basis for multistage drug delivery. Cur-Lip-TSH showed high encapsulation efficiency, suitable physicochemical properties, absence of irritation as confirmed by the HET-CAM assay, and antibacterial activity against common skin pathogens.

Overall, this platform constitutes a well-characterized and biologically safe second-generation encapsulation system that effectively addresses key physicochemical limitations of Cur for topical application. Accordingly, it provides a foundation for subsequent studies evaluating curcumin release, skin retention, permeation, and related biological activities, including antioxidant and anti-inflammatory responses, in preclinical and in vivo settings, supporting its potential use in the management of skin conditions associated with inflammation, oxidative stress, infection, and impaired tissue regeneration.

4. Materials and Methods

4.1. Chemicals

Pluronic® F-127 and curcumin (≥94%) were obtained from Sigma-Aldrich (St. Louis, MO, USA). Glycerol was purchased from Merck (Darmstadt, Germany), and sodium alginate from OregonChem (Santiago, Chile). Lipid components, including 1,2-dipalmitoyl-sn-glycero-3-phosphocholine (DPPC) and 1,2-dihexanoyl-sn-glycero-3-phosphocholine (DHPC), were acquired from Avanti Polar Lipids (Alabaster, AL, USA), while Lipoid P-100 phosphatidylcholine (>97%, non-GMO soybean) was kindly provided by Lipoid GmbH (Ludwigshafen, Germany). Cholesterol was also obtained from Sigma-Aldrich.

Ultrapure water was produced using a Thermo Scientific Barnstead MicroPure ST system (Langenselbold, Germany). Acetonitrile, methanol, isopropanol (HPLC grade), NaCl (≥99%), and 3-(4,5-dimethyl-2-thiazolyl)-2,5-diphenyl-2H-tetrazolium bromide (MTT, ≥97.5%) were supplied by Merck (Darmstadt, Germany). Sabouraud broth, tryptic soy broth, Mueller–Hinton agar, and Sabouraud agar were obtained from Becton Dickinson (Franklin Lakes, NJ, USA). Dulbecco's Modified Eagle Medium (DMEM) was purchased from Invitrogen (Thermo Fisher Scientific, Waltham, MA, USA).

4.2. Preparation of Thermosensitive Hydrogel (TSH)

TSH were prepared using Pluronic® F-127, glycerol, and alginate at varying concentrations, as detailed in Table 6. A stock solution of alginate (0.6% w/v) was prepared using deionized water, with continuous stirring for 24 h at room temperature. Glycerol was subsequently dissolved in the alginate solution at appropriate concentration, with deionized water added as required. Finally, Pluronic® F-127 was added to the mixture, which was stirred continuously at 4 °C for 24 h to ensure complete dissolution [36].

4.3. Experimental Design

4.3.1. Optimization of Thermosensitive Hydrogel (TSH)

RMS using a CCD was applied to optimize the formulation conditions of the TSH. Five experimental levels, previously defined through preliminary studies, were evaluated for each independent variable, while the responses analyzed were gelling time (s) and viscosity (mPa·s) (Table 6). The design comprised 16 experimental runs, each performed in triplicate. Experimental data were fitted to a second-order polynomial model using multiple regression analysis, and the significance of model terms was assessed by ANOVA.

Response surface and contour plots were generated to determine the optimal combination of formulation variables. All statistical analyses were conducted using Design-Expert software (version 10.0.6).

4.3.2. Gelling Time

To determine the time required for the sol–gel transition of these formulations at 34 °C, the tube inversion method described by Wang et al. [70] was employed. A 5 mL sample of the hydrogel was placed in a glass vial with a total capacity of 20 mL and an inner diameter of 2.5 mm. The vial was partially submerged (three-quarters of its length) in a water bath maintained at 34 ± 1 °C (WTB6, Memmert, Schwabach, Germany). The experiment involved monitoring the time required for the hydrogel to transition to the gel state. Gelling time was recorded by inverting the vial 180° and confirming the absence of flow in the hydrogel.

Table 6. CCD-RSM design experiment.

Variable	Code	Levels and Value				
		$-\alpha$	−1	0	+1	$+\alpha$
Independent variables (factors)						
Pluronic® F-127 (% *w*/*w*)	X_1	19.30	20.00	21.00	22.00	22.70
Glycerol (% *w*/*w*)	X_2	1.65	2.50	3.75	5.00	5.85
Alginate (% *w*/*w*)	X_3	0.10	0.20	0.35	0.50	0.60
Dependent variables (response)						
Gelation time (min)	Y_1			Minimum		
Viscosity (mPa·s)	Y_2			Maximizing		

4.3.3. Viscosity Measurements

The viscosity of the formulations was determined using a VISCO™ 895 Digital Viscometer, Package B (Atago Co., Ltd., Tokyo, Japan). A sample volume of 16 mL was maintained at a constant temperature of 22 ± 1 °C or 34 ± 1 °C, depending on the experimental conditions. All measurements were performed using needle no. 1, and viscosity values were expressed in millipascal-seconds (mPa·s).

4.4. Preparation of the Systems

4.4.1. Preparation of Cur-Loaded Liposomes

Lip was prepared by the thin-layer dispersion method [71]. Briefly, Lipoid P-100, cholesterol and Cur in a ratio of 4:1:0.1 or 4:1:1 *w*/*v* were dissolved in a chloroform into a round-bottom flask. The solvent was removed in a rotary (Büchi Rotavapor R-100, Flawil, Switzerland) at 40 °C; a thin lipid film was formed on the flask walls. The dried lipid film was rehydrated with distilled water under agitation and sonication. Cur-loaded Lip is referred to as Cur-Lip.

4.4.2. Integration of Cur and Cur-Lip on TSH Optimized

Using the optimized TSH, three different formulations were prepared (Figure 7): Blank-TSH (TSH without Cur), Cur-TSH (TSH loaded with Cur), and Cur-Lip-TSH (TSH containing Cur-Lip). For the preparation of Cur-TSH, 0.1% *w*/*w* of Cur was directly incorporated into the preformed TSH under continuous stirring until a homogeneous dispersion was obtained. In the case of Cur-Lip-TSH, Lip previously loaded with 1% *w*/*w* of Cur was mixed with the hydrogel at a 1:9 *w*/*w* ratio (Cur-Lip-TSH), result-

ing in a final Cur concentration of 0.1% w/w in the system, equivalent to that in the Cur-TSH formulation.

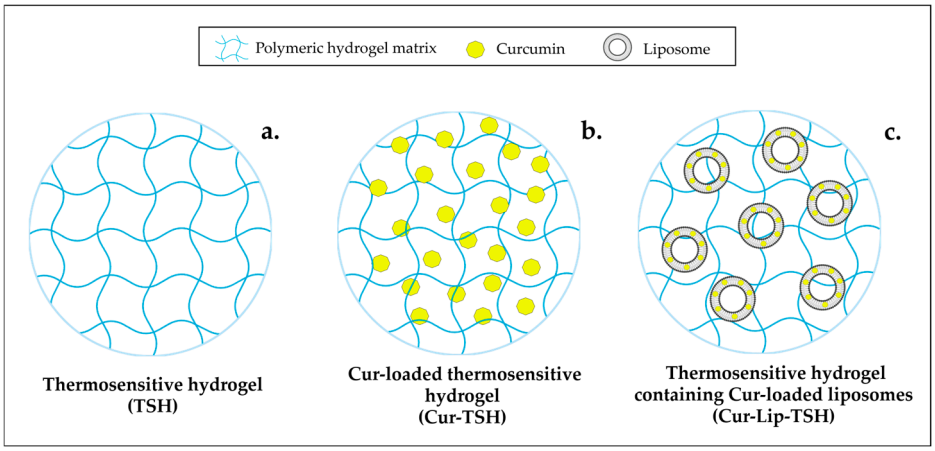

Figure 7. Schematic representation of the developed formulations: (**a**) blank thermosensitive hydrogel (TSH), (**b**) curcumin-loaded thermosensitive hydrogel (Cur-TSH), and (**c**) thermosensitive hydrogel containing curcumin-loaded liposomes (Cur-Lip-TSH).

4.5. Physicochemical Characterization of the Lipid Systems and Formulations

4.5.1. Determination of Particle Size and Polydispersity Index (PDI)

The particle size and polydispersity index (PDI) of Cur-Lip were determined using a Zetasizer Nano ZS (HT series, Malvern Instruments, Malvern, UK) at 25 °C. Measurement conditions were established according to Vergara et al. [71]. The relative refractive index, defined as the ratio between the refractive index of the phospholipids (1.490) and that of the dispersion medium (1.330), was set to 1.120, while the phospholipid absorption coefficient was fixed at 0.001.

4.5.2. Determination of Encapsulation Efficiency (EE)

To determine the percentage of Cur encapsulated in liposomes Lip, 100 µL of the formulation was centrifuged at 14,000× g for 30 min at 20 °C (Centurion Scientific Limited K2015R, Chichester, UK). After centrifugation, the supernatant was discarded, and the pellet was recovered and resuspended in a solvent mixture consisting of acetonitrile, water acidified with 2% acetic acid, and methanol (47.5:47.5:5, $v/v/v$). Cur content was quantified using a high-performance liquid chromatography (HPLC) system (Jasco, Tokyo, Japan) equipped with a quaternary pump (PU-4180), an autosampler (AS-4150), a UV–Vis photodiode array detector (MD-4010), and a C18 Inertsil® ODS-4 column (5 µm, 4.6 mm × 250 mm), operated with ChromNav software (version 2.02.08).

The mobile phase was identical to the resuspension solvent. The column temperature was maintained at 40 °C, the flow rate was set at 1 mL min^{-1}, and detection was performed at 425 nm. A 20 µL sample was injected for analysis. Cur was identified based on its retention time (9.2 min), and its concentration was determined using calibration curves constructed from Cur standards (0.5–75 ppm), yielding a correlation coefficient (R^2) of 0.99. Encapsulation efficiency (EE) was calculated according to Equation (1):

$$EE(\%) = \frac{\text{Cur loaded}}{\text{Initial amount Cur}} \times 100 \quad (1)$$

4.5.3. Extensibility (Spreadability)

The spreadability (cm^2/g) evaluation was conducted at room temperature (22 ± 1 °C) using the glass plate method, following the methodology described by Pukale et al. [72]

with some modifications. The spreadability of the TSH as a function of weight was assessed by measuring the increase in diameter. A sample of TSH equivalent to 100 mg was placed at the center of a glass plate. Another glass plate was carefully positioned on top of the sample, and a 500 g weight was placed on the upper plate. After 2 min, the weight was removed, and the diameter of the spread TSH was measured. The spreadability was calculated using the following Equation (2):

$$\text{Spreadability}\left(\text{cm}^2/\text{g}\right) = \frac{\text{A}}{\text{W}} \quad (2)$$

where: A represents the total area (cm^2) and W represents the total weight (g). Area of circle = πr^2.

4.5.4. Visual Appearance, Microscopic Studies, and pH

Formulations were visually evaluated against black and white backgrounds to assess their macroscopic appearance. Morphological characterization was carried out using scanning transmission electron microscopy (STEM, HITACHI TM4000 Plus, Tokyo, Japan) at the Nanostructured Liquids Unit (U12) of CIBER-BBN, within the ICTS NANBIOSIS facilities. The pH value of the formulation was determined using a calibrated digital pH meter Edge (Hanna Instruments, Woonsocket, RI, USA).

4.5.5. Fourier-Transform Infrared (FTIR) Spectroscopy

The chemical structure of Cur-Lip-TSH was analyzed by Fourier transform infrared (FTIR) spectroscopy using a Jasco FT-IR-4600 spectrophotometer (Jasco Corporation, Tokyo, Japan) equipped with an attenuated total reflection (ATR) accessory incorporating a ZnSe crystal positioned at a 45° incidence angle in a horizontal configuration. Spectra were recorded over the wavenumber range of 500–4500 cm^{-1} at 25 °C, with a scan speed of 20 scans s^{-1} and a spectral resolution of 16 cm^{-1}. The obtained peaks were identified and interpreted through comparison with reference spectra

4.6. Cell Culture

The human keratinocyte (HaCaT) cell line was obtained from the American Type Culture Collection (ATCC, Manassas, VA, USA) and kindly provided by the Laboratory of Biophysics of Lipids and Interfaces at the Institute of Advanced Chemistry of Catalonia (IQAC, Barcelona, Spain). All cell culture experiments were conducted at the Cell Culture Facility of IQAC.

Cells were maintained in Dulbecco's Modified Eagle Medium (DMEM) supplemented with 10% (*v*/*v*) fetal bovine serum (FBS) and 1% (*v*/*v*) penicillin–streptomycin. Cultures were incubated at 37 °C in a humidified atmosphere containing 5% CO_2. Cells were passaged at 80–90% confluence using 0.25% (*w*/*v*) trypsin–EDTA (Corning, Somerville, MA, USA) for approximately 3 min to detach adherent cells from the culture surface.

Cell Viability

The viability of human keratinocyte (HaCaT) cells following exposure to different concentrations of TSH, Cur-TSH, Cur-Lip-TSH, and free curcumin (Cur) solution was evaluated using the MTT assay. Free Cur was dissolved in DMSO. Cells were seeded at a density of 1×10^4 cells per well in a final volume of 200 µL and incubated for 24 h at 37 °C under a humidified 5% CO_2 atmosphere.

After incubation, cells were treated with TSH, Cur-TSH, Cur-Lip-TSH, or free Cur at concentrations ranging from 0.1 to 100 µM and further incubated for 24 h under the same conditions. Subsequently, the treatment media were removed, and 200 µL of MTT solution was added to each well, followed by incubation for 2 h at 37 °C. The MTT solution was

then discarded, and 100 µL of DMSO was added to each well to dissolve the formazan crystals, with the plates shaken for 5 min. Absorbance was measured at 570 nm using a microplate reader (Agilent BioTek Synergy H1, Santa Clara, CA, USA) for test, blank, and control wells. Cell viability (%) was calculated according to Equation (3).

$$\text{Cell viability } (\%) = \frac{\text{Abs}_{(sample)} - \text{Abs}_{(blank)}}{\text{Abs}_{(control)} - \text{Abs}_{(blank)}} \times 100 \quad (3)$$

where Abs represents the absorbance values of the wells with test samples, buffer medium, and untreated cells. For each experiment, the absorbance was the average value measured in a microplate reader.

4.7. In Vivo HET-CAM Assay

The hen's egg test–chorioallantoic membrane (HET-CAM) was conducted in accordance with ICCVAM guidelines [61] and Moraes de Almeida et al. [73], with minor modifications. Fresh fertilized eggs (50–60 g) were obtained from a local supplier, inspected under transillumination, cleaned, and incubated at 37 ± 1 °C and 60 ± 2% relative humidity for 8 days with automated hourly rotation. On day 8, eggs were re-examined and reincubated with the wide end oriented upward. On the following day, air chambers were marked; the marked area was incised with a scalpel and the shell carefully removed. Subsequently, 300 µL of each formulation (TSH, Cur-TSH, Cur-Lip-TSH) was applied to the exposed membrane. Sodium hydroxide 0.1% served as the positive control and sodium chloride 0.9% as the negative control. Responses were observed for 5 min and were monitored to document hemorrhage, vascular lysis, and coagulation. The onset times of the observed events were evaluated and scored according to predefined criteria: lysis was assigned scores of 5 (<0.5 min), 3 (<2 min), or 1 (<5 min); hemorrhage was scored as 7 (<0.5 min), 5 (<2 min), or 3 (<5 min); and coagulation was scored as 9 (<0.5 min), 7 (<2 min), or 5 (<5 min). The cumulative score obtained from these parameters was used to classify the irritation potential following the criteria described by Luepke [62]: ≤0.9, practically non-irritant; 1–4.9, slight irritant; 5–8.9, moderate irritant; and ≥9, strong irritant.

4.8. Antibacterial Activity

To evaluate the in vitro antimicrobial activity, *Staphylococcus aureus* ATCC 25923, *Staphylococcus epidermidis* ATCC 12228, and *Pseudomonas aeruginosa* ATCC 27853 strains were obtained from the American Type Culture Collection (ATCC). The antibacterial activity of TSH, Cur-TSH, and Cur-Lip-TSH formulations against *S. aureus*, S. epidermidis, and *P. aeruginosa* were assessed using the standard plate count method. Briefly, bacterial inoculum was cultured in tryptic soy broth (TSB) for 18 h at 37 °C. All inoculums were adjusted to a turbidity equivalent to 1×10^8 CFU/mL using the McFarland standard. Each microbial suspension was mixed with the respective formulation (TSH, Cur-TSH, or Cur-Lip-TSH) in a 1:1 ratio (*v*/*v*). A control group was prepared by replacing the formulation volume with sterile Milli-Q water. All mixtures were incubated for 24 h at 37 °C. Subsequently, 10-fold serial dilutions were prepared using sterile phosphate-buffered saline (PBS, 1% *w*/*v*), and appropriate dilutions were plated on Mueller-Hinton. Plates were incubated 24 h at 37 °C, followed by colony counting. Microbial viability was expressed as colony forming units per milliliter (CFU/mL), and the percentage of growth inhibition was calculated using the following Equation (4):

$$\text{Inhibition}(\%) = 100 - \left(\frac{\text{N} - 100}{\text{N}_0}\right) \quad (4)$$

where N represents CFU/mL of the formulation sample and N_0 represents CFU/mL of the control sample.

4.9. Statistical Analysis

Statistical analyses were performed using GraphPad Prism 9.0 software. Data from three independent experiments are expressed as mean ± standard deviation (SD). Particle size and PDI were analyzed after verifying normality and homogeneity of variances using the Shapiro–Wilk and Levene tests, respectively. Group comparisons were then performed using an independent-samples Student's *t*-test. Statistical significance was assessed using one-way ANOVA followed by Tukey's post hoc test for gelation time, viscosity, spreadability, pH, and antibacterial activity. Cell viability data were analyzed by two-way ANOVA followed by Dunnett's post hoc test, after verification of data normality. The significance level of $\alpha < 0.05$ was considered statistically significant.

Author Contributions: Conceptualization, D.V.; data curation, D.V.; formal analysis, D.V. and O.L.; funding acquisition, D.V.; investigation, D.V. and O.L.; methodology, D.V., B.V., C.S. and M.B.; project administration, D.V.; resources, D.V., O.L. and F.A.; supervision, D.V., O.L. and F.A.; validation, D.V. and B.V.; visualization, D.V.; writing—original draft preparation, D.V.; writing—review and editing, D.V. and O.L. All authors have read and agreed to the published version of the manuscript.

Funding: This research was funded by the Agencia Nacional de Investigación y Desarrollo (ANID) from the Chilean Government through FONDECYT Iniciación Project No. 11240998.

Data Availability Statement: The original contributions presented in this study are included in the article. Further inquiries can be directed to the corresponding author.

Acknowledgments: The authors thank the Center for Excellence in Translational Medicine-Scientific and Technological Bioresources Nucleus (CEMT-BIOREN) and ANID-Milenio-NCN2023_054. The authors also thank the Cell Culture Facility of the Institute of Advanced Chemistry of Catalonia (IQAC, Barcelona, Spain) and the Nanostructured Liquids Unit (U12) of CIBER-BBN at the ICTS NANBIOSIS.

Conflicts of Interest: The authors declare no conflicts of interest.

References

1. Li, J.; Mooney, D.J. Designing hydrogels for controlled drug delivery. *Nat. Rev. Mater.* **2016**, *1*, 16071. [CrossRef]
2. Zheng, J.; Song, X.; Yang, Z.; Yin, C.; Luo, W.; Yin, C.; Ni, Y.; Wang, Y.; Zhang, Y. Self-assembly hydrogels of therapeutic agents for local drug delivery. *J. Control. Release* **2022**, *350*, 898–921. [CrossRef]
3. Lavrador, P.; Esteves, M.R.; Gaspar, V.M.; Mano, J.F. Stimuli-responsive nanocomposite hydrogels for biomedical applications. *Adv. Funct. Mater.* **2021**, *31*, 2005941.
4. Kass, L.E.; Nguyen, J. Nanocarrier-hydrogel composite delivery systems for precision drug release. *Wiley Interdiscip. Rev. Nanomed. Nanobiotechnol.* **2022**, *14*, 1756.
5. Kumar, N.; Ghosh, B.; Kumar, A.; Koley, R.; Dhara, S.; Chattopadhyay, S. Multilayered "SMART" hydrogel systems for on-site drug delivery applications. *J. Drug Deliv. Sci. Technol.* **2023**, *80*, 104111.
6. Yoon, M.S.; Lee, J.M.; Jo, M.J.; Kang, S.J.; Yoo, M.K.; Park, S.Y.; Bong, S.; Park, C.-S.; Park, C.-W.; Kim, J.-S.; et al. Dual-Drug Delivery Systems Using Hydrogel–Nanoparticle Composites: Recent Advances and Key Applications. *Gels* **2025**, *11*, 520.
7. Brighenti, R.; Cosma, M.P. Mechanics of multi-stimuli temperature-responsive hydrogels. *J. Mech. Phys. Solids.* **2022**, *169*, 105045.
8. Kolawole, M.O.; Cook, M.T. *In situ* gelling drug delivery systems for topical drug delivery. *Eur. J. Pharm. Biopharm.* **2023**, *184*, 36–49. [CrossRef] [PubMed]
9. Pandey, D.K.; Kuddushi, M.; Kumar, S.; Singh, D.K. Iron oxide nanoparticles loaded smart hybrid hydrogel for anti-inflammatory drug delivery: Preparation and characterizations. *Colloids Surf. A Physicochem. Eng. Asp.* **2022**, *650*, 129631.
10. Cheng, K.; Fang, Y.; Bai, L.; Gui, F.; Ma, F.; Gao, H.; Zhao, Y.; Xu, X. Quaternized chitosan/Pluronic F127 thermosensitive hydrogel with high antibacterial properties for wound dressing. *Prog. Nat. Sci. Mater. Int.* **2023**, *33*, 581–592.

11. Soto-Garcia, P.; Antunes, S.L.; Komatsu, D.; de Alencar Hausen, M.; Dicko, C.; de Rezende Duek, E.A. Mechanical and rheological properties of Pluronic F127 based-hydrogels loaded with chitosan grafted with hyaluronic acid and propolis, focused to atopic dermatitis treatment. *Int. J. Biol. Macromol.* **2025**, *307*, 141942. [CrossRef] [PubMed]
12. Postolović, K.; Ljujić, B.; Miletić Kovačević, M.; Đorđević, S.; Nikolić, S.; Živanović, S.; Stanić, Z. Optimization, characterization, and evaluation of carrageenan/alginate/poloxamer/curcumin hydrogel film as a functional wound dressing material. *Mater Today Commun.* **2022**, *31*, 103528.
13. Abdelkader, D.H.; Elshaer, S.M.; Elkordy, E.A.; Sarhan, N.I.; Essa, E.A. Pioglitazone repurposing via in-situ gelling system: An effective topical strategy for wound management. *J. Drug Deliv. Sci. Technol.* **2025**, *106*, 106723. [CrossRef]
14. Mura, P.; Mennini, N.; Nativi, C.; Richichi, B. In situ mucoadhesive-thermosensitive liposomal gel as a novel vehicle for nasal extended delivery of opiorphin. *Eur. J. Pharm. Biopharm.* **2018**, *122*, 54–61. [CrossRef]
15. Tomić, I.; Juretić, M.; Jug, M.; Pepić, I.; Čižmek, B.C.; Filipović-Grčić, J. Preparation of in situ hydrogels loaded with azelaic acid nanocrystals and their dermal application performance study. *Int. J. Pharm.* **2019**, *563*, 249–258. [CrossRef]
16. Marzaman, A.N.F.; Sartini; Mudjahid, M.; Roska, T.P.; Sam, A.; Permana, A.D. Development of chloramphenicol whey protein-based microparticles incorporated into thermoresponsive in situ hydrogels for improved wound healing treatment. *Int. J. Pharm.* **2022**, *628*, 122323. [CrossRef]
17. Zhang, A.; Zhao, G.; Xiang, G.; Chena, R.; Donga, Y.; Diao, Q.; Wang, J.; Lin, X.; Zenga, W.; Jiang, T.; et al. Barnacle-inspired chitosan glycerin gel for skin protection and wound healing in harsh environments. *Chin. Chem. Lett.* **2025**, *36*, 110767.
18. Farshidfar, N.; Iravani, S.; Varma, R.S. Alginate-Based Biomaterials in Tissue Engineering and Regenerative Medicine. *Mar. Drugs* **2023**, *21*, 189. [CrossRef]
19. Dhayalan, M.; Wang, W.; Riyaz, S.U.M.; Dinesh, R.A.; Shanmugam, J.; Irudayaraj, S.S.; Stalin, A.; Giri, J.; Mallik, S.; Hu, R. Advances infunctional lipid nanoparticles: From drug delivery platforms to clinical applications. *3 Biotech* **2024**, *14*, 57.
20. Chen, P.; Zhang, H.; Cheng, S.; Zhai, G.; Shen, C. Development of curcumin loaded nanostructured lipid carrier based thermosensitive in situ gel for dermal delivery. *Colloids Surf. A Physicochem. Eng. Asp.* **2016**, *506*, 356–362.
21. Jain, H.; Geetanjali, D.; Dalvi, H.; Bhat, A.; Godugu, C.; Srivastava, S. Liposome mediated topical delivery of Ibrutinib and Curcumin as a synergistic approach to combat imiquimod induced psoriasis. *J. Drug Deliv. Sci. Technol.* **2022**, *68*, 103103. [CrossRef]
22. Fu, Y.S.; Chen, T.H.; Weng, L.; Huang, L.; Lai, D.; Weng, C.F. Pharmacological properties and underlying mechanisms of curcumin and prospects in medicinal potential. *Biomed. Pharmacother.* **2021**, *141*, 111888. [CrossRef]
23. Zielinska, A.; Alves, H.; Marques, V.; Durazzo, A.; Lucarini, M.; Alves, T.F.; Morsink, M.; Willemen, N.; Eder, P.; Chaud, M.V.; et al. Properties, extraction methods, and delivery systems for curcumin as a natural source of beneficial health effects. *Medicina* **2020**, *56*, 336. [CrossRef] [PubMed]
24. Vollono, L.; Falconi, M.; Gaziano, R.; Iacovelli, F.; Dika, E.; Terracciano, C.; Bianchi, L.; Campione, E. Potential of Curcumin in Skin Disorders. *Nutrients* **2019**, *11*, 2169. [CrossRef] [PubMed]
25. Gayathri, K.; Bhaskaran, M.; Selvam, C.; Thilagavathi, R. Nano formulation approaches for curcumin delivery—A review. *J. Drug Deliv. Sci. Technol.* **2023**, *82*, 104326. [CrossRef]
26. Vergara, D.; López, O.; Sanhueza, C.; Chávez-Aravena, C.; Villagra, J.; Bustamante, M.; Acevedo, F. Co-Encapsulation of Curcumin and α-Tocopherol in Bicosome Systems: Physicochemical Properties and Biological Activity. *Pharmaceutics* **2023**, *15*, 1912.
27. Zhang, Y.; Sun, B.; Wang, L.; Shen, W.; Shen, S.; Cheng, X.; Liu, X.; Xia, H. Curcumin-Loaded Liposomes in Gel Protect the Skin of Mice against Oxidative Stress from Photodamage Induced by UV Irradiation. *Gels* **2024**, *10*, 596. [CrossRef]
28. Agrawal, M.; Pradhan, M.; Singhvi, G.; Patel, R.; Ajazuddin; Alexander, A. Thermoresponsive in situ gel of curcumin loaded solid lipid nanoparticle: Design, optimization and in vitro characterization. *J. Drug Deliv. Sci. Technol.* **2022**, *71*, 103376. [CrossRef]
29. Jiang, C.; Sun, G.; Zhou, Z.; Bao, Z.; Lang, X.; Pang, J.; Sun, Q.; Li, Y.; Zhang, X.; Feng, C.; et al. Optimization of the preparation conditions of thermo-sensitive chitosan hydrogel in heterogeneous reaction using response surface methodology. *Int. J. Biol. Macromol.* **2019**, *12*, 1293–1300.
30. Craig, A.D. Temperature Sensation. In *Encyclopedia of Neuroscience*; Academic Press: Oxford, UK, 2009; pp. 903–907.
31. Hwang, T.; Jo, S.H.; Wooh, S.; Lee, H.; Jung, Y.; Yoo, J. Unveiling the Diverse Principles for Developing Sprayable Hydrogels for Biomedical Applications So-Jin Park. *Biomacromolecules* **2025**, *26*, 753–772.
32. Dumortier, G.; Grossiord, J.L.; Agnely, F.; Chaumeil, J.C. A review of poloxamer 407 pharmaceutical and pharmacological characteristics. *Pharm. Res.* **2006**, *23*, 2709–2728. [CrossRef]
33. Balan, G.A.; Precupas, A.; Matei, I. Gelation Behaviour of Pluronic F127/Polysaccharide Systems Revealed via Thioflavin T Fluorescence. *Gels* **2023**, *9*, 939. [CrossRef]
34. Lee, J.; Park, S.; Lee, S.; Kweon, H.Y.; Jo, Y.Y.; Chung, J.; Kim, J.H.; Seonwoo, H. Development of silk fibroin-based non-crosslinking thermosensitive bioinks for 3D bioprinting. *Polymers* **2023**, *15*, 3567.
35. Sarkhel, S.; Jaiswal, A. Emerging Frontiers in In Situ Forming Hydrogels for Enhanced Hemostasis and Accelerated Wound Healing. *ACS Appl. Mater. Interfaces* **2024**, *16*, 61503–61529. [CrossRef]

36. Lupu, A.; Gradinaru, L.M.; Rusu, D.; Bercea, M. Self-healing of Pluronic® F127 hydrogels in the presence of various polysaccharides. *Gel* **2023**, *9*, 719.
37. Badruddoza, A.Z.M.; Zahid, M.I.; Walsh, T.; Shah, J.; Gates, D.; Yeoh, T.; Nurunnabi, M. Topical drug delivery by Sepineo P600 emulgel: Relationship between rheology, physical stability, and formulation performance. *Int. J. Pharm.* **2024**, *658*, 124210. [CrossRef] [PubMed]
38. Ferreira, A.; Ferreira, L.; Pelosine, A.M.; Alves, W.A.; Ribeiro, D. Tuning Pluronic Hydrogel Properties via Ionic Strength and Hyaluronic Acid for Optimized Rheology and Drug Delivery Performances. *ACS Omega* **2025**, *10*, 60519–60531. [CrossRef] [PubMed]
39. Zakaria, A.S.; Afifi, S.A.; Elkhodairy, H.A. Newly Developed Topical Cefotaxime Sodium Hydrogels: Antibacterial Activity and In Vivo Evaluation. *Biomed Res. Int.* **2016**, 6525163.
40. Chow, P.S.; Lim, R.T.Y.; Cyriac, F.; Shah, J.C.; Badruddoza, A.Z.M.; Yeoh, T.; Yagnik, C.K.; Tee, X.Y.; Wong, A.B.H.; Chia, V.D.; et al. Influence of manufacturing process on the microstructure, stability, and sensorial properties of a topical ointment formulation. *Pharmaceutics* **2023**, *15*, 2219. [CrossRef]
41. Kumari, P.; Kant, V.; Ahuja, M. Formulation, characterization, in vitro and in vivo evaluation of thermoresponsive lawsone-based Pluronic F-127 nanogels for wound healing. *J. Drug Deliv. Sci. Technol.* **2024**, *93*, 105451. [CrossRef]
42. Bąk-Kuchejda, U.; Witczak, T.; Witczak, M.; Krupa, A. The impact of semisolid matrices on spreadability, rheology and celecoxib release rate. *Polim Med.* **2025**, *55*, 49–58. [CrossRef] [PubMed]
43. Akhtara, F.; Kobra, K.; Wong, S.Y.; Li, X.; Arafat, M.T. Glycerol crosslinked vitamin E loaded xanthan gum and gellan gum nanoemulgels for topical management of dry skin. *Int. J. Biol. Macromol.* **2025**, *333*, 148769. [CrossRef]
44. Wang, E.; Qi, Z.; Cao, Y.; Li, R.; Wu, J.; Tang, R.; Gao, Y.; Du, R.; Liu, M. Gels as Promising Delivery Systems: Physicochemical Property Characterization and Recent Applications. *Pharmaceutics* **2025**, *17*, 249. [CrossRef] [PubMed]
45. Paswan, M.; Singh Chandel, A.K.; Malek, N.I.; Dholakiya, B.Z. Preparation of sodium alginate/Cur-PLA hydrogel beads for curcumin encapsulation. *Int. J. Biol. Macromol.* **2024**, *254*, 128005. [CrossRef] [PubMed]
46. Chen, Y.; Sathiyaseelan, A.; Zhang, X.; Jin, Y.; Wan, M.H. Preparation of antibacterial tellurium nanorod-incorporated thermosensitive pluronic F-127 hydrogels for wound healing applications. *J. Drug Deliv. Sci. Technol.* **2025**, *111*, 107107. [CrossRef]
47. Alaee, R.; Mohammadi, T.; Mahinroosta, M. pH-responsive xanthan-glycerol hydrogel: An effective wound dressing for controlled amoxicillin delivery. *Int. J. Biol. Macromol.* **2025**, *318*, 145112. [CrossRef]
48. Sharma, A.; Verma, C.; Mukhopadhyay, S.; Gupta, A.; Gupta, B. Development of sodium alginate/glycerol/tannic acid coated cotton as antimicrobial system. *Int. J. Biol. Macromol.* **2022**, *216*, 303–311. [CrossRef]
49. Zhou, R.; Fangfang, N.; Wu, S.; Wang, X.; Ming, J.; Zhang, L.; Dong, L.; Song, Z.; Ren, G.; Huang, M.; et al. Preparation and mechanism of Lactobacillus plantarum and curcumin co-encapsulated in alginate-gelatin hydrogel beads. *Food Chem.* **2025**, *493*, 145995. [CrossRef] [PubMed]
50. Mostajeran, N.; Kamali, H.; Arabi, L.; Movaffagh, J.; Alavizadeh, S.H.; Mohammadzadeh, V.; Rahiman, N.; Shahri, M.K.; Jaafari, M.R.; Mohammadi, M. Thermosensitive hydrogel containing liposomal nanoparticles of deferoxamine and curcumin: In vitro evaluation and diabetic wound healing effect in rats. *Int. J. Pharm.* **2025**, *685*, 126227. [CrossRef]
51. Calderon-Jacinto, R.; Matricardi, P.; Gueguen, V.; Pavon-Djavid, G.; Pauthe, E.; Rodriguez-Ruiz, V. Dual Nanostructured Lipid Carriers/Hydrogel System for Delivery of Curcumin for Topical Skin Applications. *Biomolecules* **2022**, *12*, 780. [CrossRef]
52. Kalantarnia, F.; Maleki, S.; Shamloo, A.; Akbarnataj, K.; Tavoosi, S.N. A thermo-responsive chitosan-based injectable hydrogel for delivery of curcumin-loaded polycaprolactone microspheres to articular cartilage: In-vitro and in-vivo assessments. *Carbohydr. Polym. Technol. Appl.* **2025**, *9*, 100678. [CrossRef]
53. Demol, J.; Lambrechts, D.; Geris, L.; Schrooten, J.; Van Oosterwyck, H. Towards a quantitative understanding of oxygen tension and cell density evolution in fibrin hydrogels. *Biomaterials* **2011**, *32*, 107–118. [CrossRef] [PubMed]
54. Slavkova, M.; Lazov, C.; Spassova, I.; Kovacheva, D.; Tibi, I.P.-E.; Stefanova, D.; Tzankova, V.; Petrov, P.D.; Yoncheva, K. Formulation of Budesonide-Loaded Polymeric Nanoparticles into Hydrogels for Local Therapy of Atopic Dermatitis. *Gels* **2024**, *10*, 79. [CrossRef]
55. Cîrloiu, G.-S.; Segneanu, A.-E.; Bejenaru, L.E.; Văruţ, M.C.; Bălăşoiu, R.M.; Călina, D.; Stoian, A.-C.; Băluşescu, G.; Herea, D.-D.; Ciocîlteu, M.V.; et al. Sprayable Hybrid Gel with Cannabidiol, Hyaluronic Acid, and Colloidal Silver: A Multifunctional Approach for Skin Lesion Therapy. *Pharmaceutics* **2025**, *17*, 1189. [CrossRef] [PubMed]
56. Arpa, M.D.; Biltekin Kaleli, S.N. Thermosensitive Sprayable Lidocaine–Allantoin Hydrogel: Optimization and In Vitro Evaluation for Wound Healing. *Pharmaceutics* **2025**, *17*, 1607. [CrossRef] [PubMed]
57. Chen, H.; Zhang, Z.; Qi, J.; Cao, C.; Lin, M.; Lyu, L.; Xu, D. Novel Thermosensitive Hydrogel Encapsulated Carvedilol for the Treatment of Rosacea. *ACS Omega* **2025**, *19*, 7964–7972. [CrossRef]
58. Fernández-Romero, A.-M.; Maestrelli, F.; García-Gil, S.; Talero, E.; Mura, P.; Rabasco, A.M.; González-Rodríguez, M.L. Preparation, Characterization and Evaluation of the Anti-Inflammatory Activity of Epichlorohydrin-β-Cyclodextrin/Curcumin Binary Systems Embedded in a Pluronic®/Hyaluronate Hydrogel. *Int. J. Mol. Sci.* **2021**, *22*, 13566. [CrossRef] [PubMed]

59. Zhou, Q.; Cai, X.; Huang, Y.; Zhou, Y. Pluronic F127-liposome-encapsulated curcumin activates Nrf2/Keap1 signaling pathway to promote cell migration of HaCaT cells. *Mol. Cell. Biochem.* **2023**, *478*, 241–247. [CrossRef]
60. Martins, J.R.T.L.; Vaz, G.R.; Vaiss, D.P.; Yurgel, V.; Dias, D.C.C.; Madruga, S.; Farias, B.S.; Cadaval, T.R.S.; Pinto, L.A.A.; Domagalski, J.L.; et al. Designing and characterization of hydrogels containing curcumin and polyhexamethylene biguanide for wound healing: In vitro pharmacological evaluation. *J. Mol. Liq.* **2025**, *437*, 128389. [CrossRef]
61. ICCVAM-Recommended Test Method Protocol: Hen's Egg Test-Chorioallantoic Membrane (HET-CAM) Test Method. (n.d.). Available online: https://ntp.niehs.nih.gov/sites/default/files/iccvam/docs/protocols/ivocular-hetcam.pdf (accessed on 6 February 2026).
62. Luepke, N. Hen's egg chorioallantoic membrane test for irritation potential. *Food Chem Toxicol.* **1985**, *23*, 287–291. [CrossRef]
63. Ling, Y.; Wang, Y.; Cai, Y.; Zhao, S.; Liu, H. Preparation of Multifunctional Hydrogel with Curcumin-Controlled Release and Photothermal Synergistic Antibacterial Property for Wound Dressing. *Ind. Eng. Chem. Res.* **2025**, *64*, 19876–19889. [CrossRef]
64. Patel, H.S.; Saxena, I.; Bhargriya, P.N.; Makwana, B.B.; Parmar, H.A.; Sharma, R.K. Development and Evaluation of Curcumin-Loaded Pluronic-Polyvinyl Alcohol hydrogel Systems: Synthesis, Characterization, Biological and Computational Investigations. *BioNanoScience* **2025**, *1*, 553. [CrossRef]
65. Dai, C.; Lin, J.; Li, H.; Shen, Z.; Wang, Y.; Velkov, T.; Shen, J. The Natural Product Curcumin as an Antibacterial Agent: Current Achievements and Problems. *Antioxidants* **2022**, *11*, 459. [CrossRef]
66. Stachowiak, M.; Mlynarczyk, D.T.; Dlugaszewska, J. Wondrous Yellow Molecule: Are Hydrogels a Successful Strategy to Overcome the Limitations of Curcumin? *Molecules* **2024**, *29*, 1757. [CrossRef]
67. Braido, B.; Rukavina, Z.; Grimstad, Ø.; Franzè, S.; Cilurzo, F.; Vanić, Ž.; Škalko-Basnet, N.; Hemmingsen, L.M. Liposomes-in-hydrogel for topical drug delivery: Mechanical, kinetic, and biological insights. *J. Drug Deliv. Sci. Technol.* **2025**, *113*, 107380. [CrossRef]
68. Sharun, K.; Nair, S.S.; Banu, S.A.; Manjusha, K.M.; Jayakumar, V.; Saini, S.; Pawde, A.M.; Kumar, R.; Dhama, K.; Pal, A. In vitro Antimicrobial Properties of Pluronic F-127 Injectable Thermoresponsive Hydrogel. *J. Pure Appl. Microbiol.* **2023**, *17*, 1231–1237. [CrossRef]
69. Hao, P.Y.; Zhou, H.Y.; Ren, L.J.; Zheng, H.J.; Tong, J.N.; Chen, Y.W.; Park, H.J. Preparation and antibacterial properties of curcumin-loaded cyclodextrin-grafted chitosan hydrogel. *J. Sol-Gel Sci. Technol.* **2023**, *106*, 877–894. [CrossRef]
70. Wang, W.; Wat, E.; Hui, P.; Chan, B.; Ng, F.; Kan, C.; Wang, X.; Hu, H.; Wong, E.; Lau, C.; et al. Dual-functional transdermal drug delivery system with controllable drug loading based on thermosensitive poloxamer hydrogel for atopic dermatitis treatment. *Sci. Rep.* **2016**, *6*, 24112. [CrossRef]
71. Vergara, D.; Shene, C. Encapsulation of lactoferrin into rapeseed phospholipids based liposomes: Optimization and physicochemical characterization. *J. Food Eng.* **2019**, *262*, 29–38. [CrossRef]
72. Pukale, S.S.; Sharma, S.; Dalela, M.; Singh, A.K.; Mohanty, S.; Mittal, A.; Chitkara, D. Multi-component clobetasol-loaded monolithic lipid-polymer hybrid nanoparticles ameliorate imiquimod-induced psoriasis-like skin inflammation in Swiss albino mice. *Acta Biomater.* **2020**, *115*, 393–409. [CrossRef]
73. de Almeida, T.M.; Kudrna, K.B.; Biasuz, E.; Spiazzi, C.C.; Felix, I.R.; Leite, D.C.; Cossetin, L.F.; Librelotto, D.R.N.; Schaffazick, S.R.; de Bona da Silva, C. Ferulic acid-loaded Nanoemulsion Gels: A strategy for enhanced skin delivery and reduced irritation. *J. Drug Deliv. Sci. Technol.* **2025**, *11*, 107199. [CrossRef]